Synthesis and characterization of innovative resveratrol nanobelt-like particles and assessment of their bioactivity, antioxidative and antibacterial properties

Nina Tomić[1], Tamara Matić[2], Nenad Filipović[1], DraganaMitić Ćulafić[3], Aldo R. Boccacccini[4], Magdalena M. Stevanović[1*]

[1]Group for Biomedical Engineering and Nanobiotechnology, Institute of Technical Sciences of SASA, Belgrade, Serbia, KnezMihailova 35/IV 11000 Belgrade, Serbia

[2]Innovation Center of the Faculty of Technology and Metallurgy Ltd, Karnegijva 4, Belgrade, Serbia

[3]Faculty of Biology, University of Belgrade, Studentski trg 16, Belgrade, Serbia

[4]Institute of Biomaterials, Department of Materials Science and Engineering, University of Erlangen-Nuremberg, 91058 Erlangen, Germany

Abstract

Recently, many studies have shown various beneficial effects of polyphenol resveratrol (Res) on human health. The most important of these effects include cardioprotective, neuroprotective, anti-cancer, anti-inflammatory, osteoinductive, and anti-microbial effects. Resveratrol has cis and trans isoforms, with the trans isoform being more stable and biologically active. Despite the results of *in vitro* experiments, resveratrol has limited potential for application *in vivo* due to its poor water solubility, sensitivity to oxygen, light, and heat, rapid metabolism, and therefore low bioavailability. The possible solution to overcome these limitations could be the synthesis of resveratrol in nanoparticle form. Accordingly, in this study, we have developed a simple, green solvent/non-solvent

[*] Corresponding author: Magdalena M. Stevanović E-mail: magdalena.stevanovic@itn.sanu.ac.rs

physicochemical method to synthesize stable, uniform, carrier-free resveratrol nanobelt-like particles (ResNPs) for applications in tissue engineering. UV–visible spectroscopy (UV-Vis) showed good stability of the active resveratrol isoform in the particles. The activeform was also confirmed by Fourier transform infrared spectroscopy (FTIR) and X-ray diffraction (XRD). Nanobelt-like morphology was observed by optical microscopy and field-emission scanning electron microscope (FE-SEM). Bioactivity was confirmed using *Artemia salinain vivo* toxicity assay, while 2,2–diphenyl-1-picrylhydrazylhydrate (DPPH) reduction assay showed the good antioxidative potential of concentrations of 100 µg/ml and lower. Microdilution assay on several reference strains and clinical isolates showed promising antibacterial potential on *Staphylococci*, withminimal inhibitory concentration (MIC) being 800 µg/ml.Bioactive glass-based scaffolds were coated with ResNPs and characterized to confirm coating potential. All of the above make these particles a promising bioactive, easy-to-handle component in various biomaterial formulations.

Keywords: resveratrol, nanoparticles, bioactivity assay, antioxidative activity, antibacterial activity

1. Introduction

Many of the new drugs, especially among phytopharmaceuticals, are poorly water-soluble and hence have low bioavailability.[1] Resveratrol is hydrophobic (solubility <0.05 mg/mL), undergoes fast metabolization in the intestines and liver,[2] and is also a highly reactive and therefore unstable molecule owing to the presence of OH-groups, benzene rings, and C=C bonds.[3] Resveratrol is stable in acidic conditions but starts to degrade exponentially above

pH 6.8, reaching maximum degradation at pH 9.[4] When exposed to light, trans-resveratrol goes through a configuration change to cis form, which has no significant biological activity.[3] All of this, combined with heat lability, makes resveratrol short-lived and impractical for *in vivo* use.[2,4,5] There have already been efforts to prepare resveratrol delivery systems capable of sustained release of this compound.[2,5] Among nanoformulations, nanofibers, and similar structures are of particular interest in tissue engineering.[6]Riccitello et al.[7]showed an effect of poly(ε-caprolactone) and poly(lactic) acid-loaded resveratrol nanofibers on bone cells, while Lin et al.[8]synthesized resveratrol-loaded polyvinylpyrrolidone/cyclodextrin nanofibers for topical application. Zhang et al.[9]achieved thesustained release of resveratrol and xanthohumol from polyethylene oxide/poly(lactide-co-glycolide) fibres. These studies relied on the electrospinning technique to obtain nanofibers. The majority of the methods for creating resveratrol nanoformulations rely on different additives to ensure adequate stability and solubility of micro- and nanoparticles.[2] Limitations to this approach include thedemanding process of synthesis, toxicity of surfactants used to disperse thedrug, expensive polymers for incorporation, or poor loading capacity. Bioavailability of resveratrol can also be improved by thesynthesis of pure resveratrol particles, using asupercritical antisolvent process.[10] Furthermore, Jangid et al.[11]synthesized carrier-free resveratrol nanoparticles by ultrasonic method, using only 0,5% sodium dodecyl sulfate.

One of the promising applications of polyphenols and generally nature-derived compounds is as antioxidants in tissue engineering.[12,13] Polyphenols induce a reduction of free radicals, preventing tissue damage, and possess multiple other beneficial biological activities, which are being increasingly studied.[12–14] Resveratrol in particular has been suggested to promote the survival of bone cells via multiple mechanisms,[14,15] it has a positive effect on the prevention of bone density loss[16] and antibacterial and antifungal activity.[17,18] However, the

treatment of bone defects still remains a great challenge, especially for those defects associated with vascular and nerve injuries.[19] Most research related to bone tissue engineering isfocused on osteogenic cell differentiation. The reason is the lack of suitable materials and methodology which will mimic the natural matrix and also consider the formation of blood vessels and nerves in the newly formed bone. Nanobelt-like structures achieve better biocompatibility and more effective interactions with the interface of the tissue compared to materials that are already in use in clinical practice which possess limitations reducing their therapeutic effects.[20] There are recent examples of nanobelt-like structures serving as a cell multilineage differentiation platform for biomimetic construction of bioactive 3D osteoid tissue *in vitro.*[19]

Here we present a simple method of synthesizingcarrier-free Res nanobelt-like particles (ResNPs) without the use of hazard additives or solvents in the synthesis. The newly synthesized ResNPs were characterized by UV-Vis, FTIR, XRD, optical microscopy, and SEM. To assess the bioactivity of ResNPs, we used aeukaryotic *in vivo* test system in theform of brine shrimp, *Artemia salina,* and performed aDPPH assay to show antioxidative activity.We also tested ResNPs for effects on the following bacterial strains: *Staphylococcus aureus*, *Escherichia coli*, *Pseudomonas aeruginosa*, *Staphylococcus epidermidis*, *Enterococcus faecalis*, *Proteus mirabilis*, ATCC strains and several clinical strains from hospital-associated infections (one strain *of S. aureus, S. epidermidis, E. coli,* and *P. aeruginosa*). In addition, the potential of ResNPs for the coating of bioactive glass-based scaffolds was examined, to show theadvantages of this form regarding thepractical application of resveratrol.

2. Materials and methods

2.1. Materials

The reagents used were of analytical grade, trans-resveratrol (≥98% ChromaDex (Irvine, CA, USA), ethanol (96% Zorka Pharma, Serbia), methanol (99.5% Zorka Pharma, Serbia), Mueller Hinton broth (Torlak, Serbia), streptomycin (Thermo Fisher Scientific, USA) resazurin sodium salt (Sigma-Aldrich, St. Louis, MO, USA), 2,2–diphenyl-1-picrylhydrazylhydrate (DPPH) (Sigma-Aldrich (St. Louis, MO, USA), NaCl (Centrohem, Serbia). *Artemia salina* eggs were from Dajana Pet, Czech Republic. 45S5 Bioglass® powder, PVA (Merck, Darmstadt, Germany), and polyurethane (PU) foam (Eurofoam Deutschland GmbH) were used for scaffold fabrication.

2.2. Synthesis of resveratrol nanobelt-like particles (ResNPs)

ResNPs were prepared using a simple solvent/nonsolvent physicochemical method (**Figure 1**). Firstly, 50 mg of trans-resveratrol powder was dissolved in 5 ml of 96% ethanol. The obtained solution was added drop-wise into 25 ml of precooled water (5^{o}C) during 5 min of high-speed homogenization at 17500 rpm. Afterward, the suspension was protected from the light and stored at 4^{o}C. One part of the suspension was dried for48h in a laminar chamber (Chemland, Poland), at ambient temperature for characterization purposes while the other was left for the stability study.

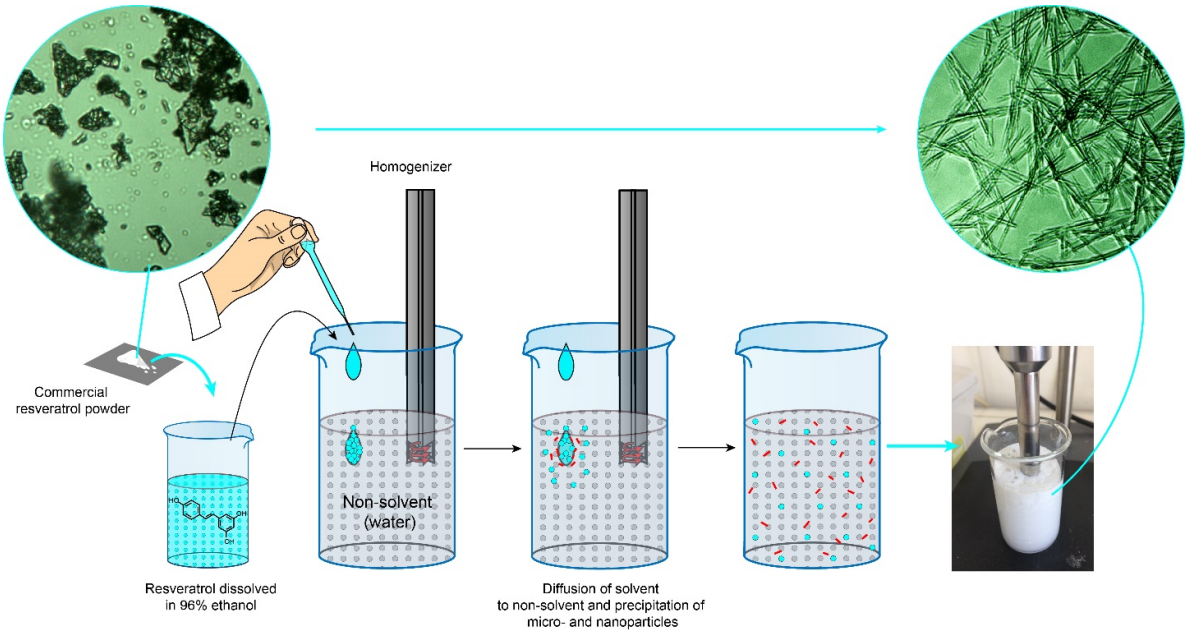

Figure 1. Scheme representing the synthesis of nanobelt-like ResNPs

2.3. Characterization of ResNPs

2.3.1. UV-Vis spectroscopy

UV measurements were performed to confirm the quality composition of the samples *i.e.* trans isoform of resveratrol. This was done on a GBC Cintra UV–Vis spectrophotometer in the wavelength range of 260–600 nm. The spectra were recorded at room temperature, with a standard quartz cuvette cell path length (10mm).

2.3.2. Fourier transform infrared spectroscopy

The quality analysis of the samples was also performed by FTIR spectroscopy. The FTIR spectrum was recorded on spectrometer Nicolet iS10 (Thermo Fisher Scientific, Waltham, MA, USA), using attenuated total reflectance (ATR) mode. Measurements were performed

in a spectral range of 400–4000 cm^{-1} with a resolution of 4 cm^{-1} and the number of scans was 32.

2.3.3. X-ray diffraction

To further investigate the structural characteristics of the samples, XRD spectra were obtained on an X-ray diffractometer, Philips PW 1050 diffractometer with Cu-Kα radiation (Ni filter). The samples were scanned in the 2θ range of 5° to 70°, with a scanning step width of 0.05°, and 2 s per step.

2.3.4. Optical microscopy

Sample surface*i.e.*morphology of ResNPshas been investigated under 200, 500, and 1000x magnification by OPTICA B-500MET light microscope (Optica SRL, Italy) using Optica Vision Pro software. Three drops of suspension or a sample of dry powder were smeared on microscope slides and images werecollected with OPTIKAM PRO 8LT – 4083.18 camera equipped with a scientific-grade CCD sensor.

2.3.5. Field-emission scanning electron microscope

The closer insight into themorphology of ResNPs was determined by Tescan Mira 3 XMU FE-SEM operated at 20 keV. Prior to imaging ResNPs suspension was applied at the metallic stub, air-dried for 24h, and sputter-coated with a thin layer of gold. The mean length and width of particles weredetermined from the micrographs by using the ImageJ software.

2.4. Artemia salina bioassay for determination of the bioactivity

It is of great importance to confirm if novel materials are indeed bioactive as expected. *Artemia salina* bioassay is a widely used assay.[21,22] However, only recently it has been used for the determination of the biological effects of nanomaterials.[23] The biological activity of ResNPswas evaluated by a slightly modified procedure described by Rajabi et al.[23]*Artemia salina* eggs were incubated overnight in 3,5% pre-filtered saline water at 30^{o}C, under constant illumination and intensive aeration, as a slight modification of the procedure described by Rajabi et al.[23] 2h upon start of hatching, nauplii (larval Instar I phase) were separated from unhatched eggs and eggshells, allowing same age of nauplii.[24] 6 nauplii per well were sorted in 96 well plates (16 wells per concentration in each replicate) and treated with 0.1-375 µg/ml of ResNPs suspension, by adding 50 µl of ResNPs suspension to 150 µl of saline water with nauplii. Surviving nauplii were counted after 24h or 48h using DigiMicro 2.0. Scale and AMCap software. The volume of ethanol equivalent to the amount in the highest ResNPs concentration was used to treat the first treatment group. *Artemia* larvae were considered dead if no movement was observed during the 15s of observation, and numberof survivals was compared to the negative control group. LD_{50} value was counted using Probit analysis.[25]

2.5. DPPH reduction assay

DPPH is a stable nitrogen radical that can accept hydrogen cation transferred from the molecules with antioxidant activity, which leads to the change of purple color of DPPH solution to yellow, and to the decrease of characteristic absorbance peak at 517nm.[13,26]In order to assess the antioxidative potential in methanol and water, the percentage of reduction of DPPH by ResNPs was measured by using absorbance at 517nm on UV-Vis.

Ascorbic acid was used as a positive control. ResNPs, commercial resveratrol, and ascorbic acid were dispersed in methanol or water. DPPH was dissolved in methanol at a concentration of 200 µM using an ultrasonic bath and protected from light. 200 µl of DPPH was added to 800 µl of samples. The finalconcentrations of test samples were 1mg/ml, 100, 10, and 1 µg/ml. Following the addition of DPPH solution, each sample was incubated for 30 min. Then, the absorbance was measured in the wavelength range of 400 to 650 nm on a GBC Cintra UV–Vis spectrophotometer.

DPPH scavenging activity was calculated using theformula:

$$\text{Scavenging activity (\%)} = 100 * (A_C - A_S) / A_C$$

With control value (A_C) being the absorbance of non-reduced DPPH after 30 min of incubation, and A_S absorbance of the sample.

2.6. *Antimicrobial activity*

Antibacterial activity was assessed on several Gram-negative and Gram-positive bacterial species. All bacteria were provided by the Institute for microbiology and immunology, University of Belgrade – Faculty of Medicine, Belgrade, Serbia**.** Bacteria were chosen to be representatives of species relevant tocauses of tissue implant infections. Among these, the most notable are strains of *Staphylococcus aureus* and *S. epidermidis*, which represent the main cause of tissue implant infections.[27]

MIC and minimal bactericidal concentration (MBC) were investigated by microdilution assay and resazurin stain. For each experiment, bacterial cultures were freshly prepared by overnight incubation in Mueller Hinton broth (MHB) in a shaker incubator at 37^{o}C. The

numberof bacteria was adjusted to 10^8 CFU/ml using OD_{600} measurements, and then diluted to 10^6 CFU/ml in 0.01M $MgSO_4$.

MIC assay was set by preparing serial two-fold dilutions of test substances in growth media, in the columns of a 96-well microtiter plate. Commercial resveratrol powder and ResNPs were tested in theconcentration range of 6.25 - 800 µg/ml, and streptomycin was used as positive antibiotic control in the range of 0.78 - 100 µg/ml. Color control and solvent (water-ethanol) control of according volumes were also prepared by serial dilutions. 20 µl of bacterial inoculum, containing $2x10^4$ CFU was added to each well (final volume 200 µl per well), and plates were incubated for 24h at 37°C. Then, 22 µl of resazurin (aqueous solution of 0.675 mg/ml) was added to each well of the microtiter plate, and plates were incubated for 2h. MIC values were established as the lowest concentration of test substance in the wells exhibiting no change of color of indicator dye. In order to check for MBC values, samples from wells showing no visible growth were plated to Mueller Hinton agar plates, followed by incubation at 37°C. For each strain, experiments were performed for three individual times.

2.7. ResNPs coating of bioactive glass-based scaffold

45S5 Bioglass® scaffolds were prepared by foam replica method.[28] The coating was performed using the rotary evaporator (IKA RV8) by immersing the scaffolds into 4 ml of ResNPs suspension followed by rotation (60rpm) and solvent evaporation at 45°C and vacuum. After 20 min of coating, the scaffolds were placed on the filter paper and left to dry under the laminar hood for 4h. The quality of the coating was estimated using FTIR analysis and optical microscopy.

2.8. Statistical analysis

All experiments were done in triplicate, and statistical analysis was performed using Origin Software (OriginLab Corporation) and Microsoft Excel (Microsoft). Results of scavenging activity among ResNPs and commercial resveratrol were compared using student'st-test and the statistical significance threshold was p-value <0.05.

3. Results and discussion

3.1. UV-Vis, FTIR, and XRD characterization

The formation of ResNPs became visible during high-speed homogenization by the appearance of white colorization. The UV spectroscopy results shown in **Figure 2A** indicated the formation of the trans isoform of resveratrol particles. Biologically active trans-resveratrol undergoes conformation change to inactive cis isoform when exposed to light.[3] The difference between these two isoforms can be seen from UV-Vis spectra by λ_{max}since trans-resveratrol has a redshift by 30 nm.[29] From the literature, absorbance peaks of trans-resveratrol are distinct around 320 nm and 305 nm, while cis-resveratrol has an absorption maximum between 280 and 295 nm.[30] Therefore, we used this method to monitor if conformation change happened in our ResNPs suspension during experimental work or subsequent storage. UV-Vis spectrum displayed a narrow surface absorption band at λ=310 nm characteristic oftrans-resveratrol (**Figure 2A**). Measurement of freshly made suspension showed UV-Vis spectrum with thesame band position as suspension 63 days after synthesis indicating good stability of the sample.

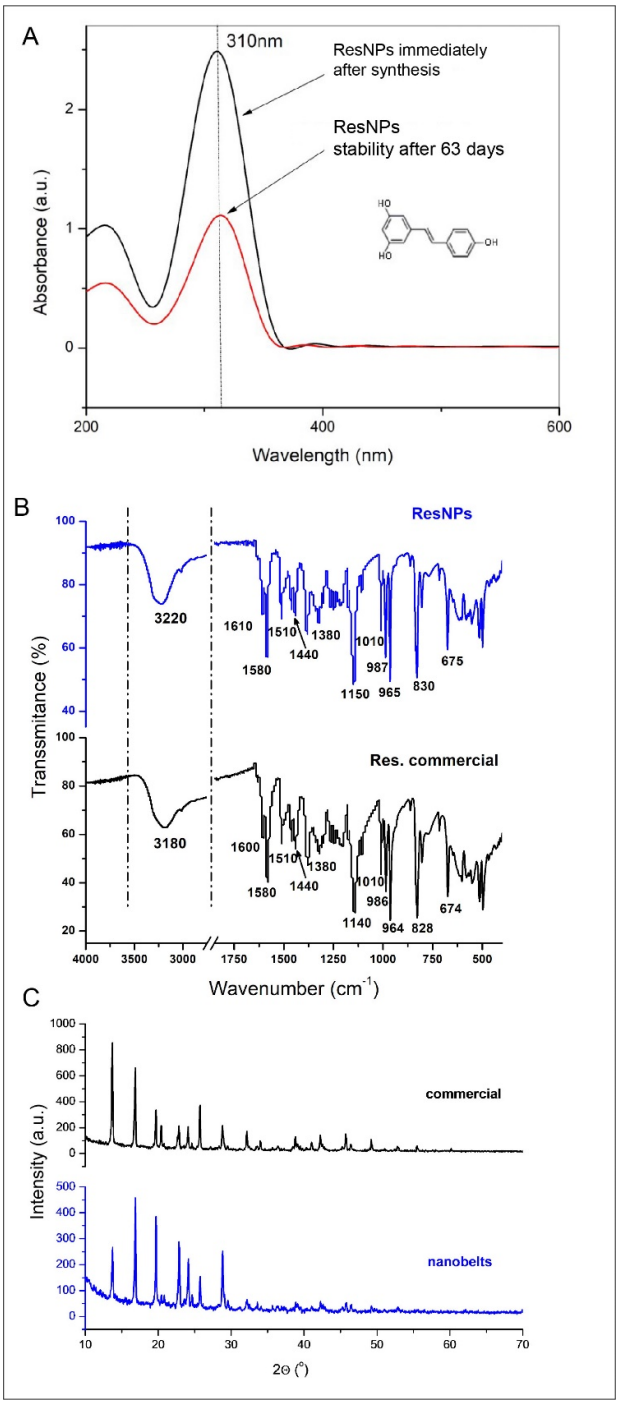

Figure 2. A) UV-Vis spectrum of ResNPs immediately after synthesis and 63 days later. B) FTIR spectra of as-prepared nanobelt-like ResNPs and commercial resveratrol. C) XRD patterns of nanobelt-like ResNPs and commercial resveratrol

The FTIR spectra of commercial Res and ResNPs are presented in **Figure 2B.** Both spectra exhibit peaks characteristic for Res without significant difference between them. In the lower wavenumber region, the most dominant peaks correspond to the vibrations of benzene rings (several peaks between 1610-1440 cm^{-1}), the in-plane bending vibrations of C-H and OH bonds as well as stretching of C-C from the vinylidene group (1380-1180 cm^{-1}), the vibrations of C-O bonds (1150-1010 cm^{-1}), out-of-plane bending vibrations of C-H bonds (980-830 cm^{-1}, among them band at 965 cm^{-1} is specific for the trans-Res) and out-of-plane deformational vibration of OH group (675 cm^{-1}).[31,32] In the higher wavenumber region, the dominant broad peaks originated from OH vibrations. In fact, in this region is observed only difference between spectra as a band shifting from 3180 to 3220 cm^{-1}. The possible explanation for this phenomenon could be correlation with a difference in the amount of intermolecular hydrogen bonding as a consequence of nanobelt structure. The thickness of nanobelts was significantly smaller than random agglomerates in the commercial sample and thus hydroxyl groups wereless influenced by electronegative O from thenearest molecules.

The crystalline nature of ResNPs was determined by XRD from obtained powders (**Figure 2C**). For comparison purposes, the diffractogram of commercial Res was given as well. Several sharp, intensive diffraction peaks were recorded at the following 2θ angles: 13.75, 16.85, 19.7, 22.85, 24.15, 25.75, and 28.85. These results are in good agreement with previously reported patterns for Res monoclinic form, with a slightly lower position of 2θ angles, 0.4 ° onaverage.[32,33] Although positions of the diffraction peaks in the commercial and nanobelt form of Res are the same, significant difference can be observed regarding their intensity. For example, the most intense peak in the commercial sample was recorded

at 13.75 °, while this peak is fifth by the intensity in the nanobelt form. As R. Chadha et al.[33]reported in their thorough investigation ofRes crystalline structure, this compound exhibited several polymorphic forms with a significant difference in crystal morphology and aspect ratio. When it comes to nanobelts form, it was expected that ResNPs crystals possess different total areas of each facet responsible for the diffraction of incident X-rays. The effects of crystalline form on various physicochemical properties such as solubility, bioavailability, and thus theefficacy of the solid drugs have been proven in the past.[34,35] While thethermodynamically most stable form guarantees solid long-term stability, other polymorphic forms could be beneficial regarding solubility and bioavailability.

3.2. Morphological characterization

Morphology presents one of the most important parameters which determine the way a nanomaterial interacts with the tissue, and consequently how effective the material would be for therapeutic purposes. The size, shape, and composition of the particles are mostly influenced by the synthesis parameters, and the presence of reducing or stabilizing agents, additives, etc. The ResNPs in this study were obtained by a very simple solvent/nonsolvent physicochemical method and without the use of agents or additives in the synthesis process. The morphology of the obtained ResNPs, as determined by the optical and scanning electron microscope is shown in **Figure 3B**. The particles were uniform, showing thetendency of grouping to bigger fascicles. The obtained nanobelt-like ResNPshad a large width-to-thickness ratio. The mean length, as measured by ImageJ from optical microscopy images, was around 17 µm **(Figure 3B)**, and the mean width, from SEM micrographs 750 nm (**Figure 3C**.).

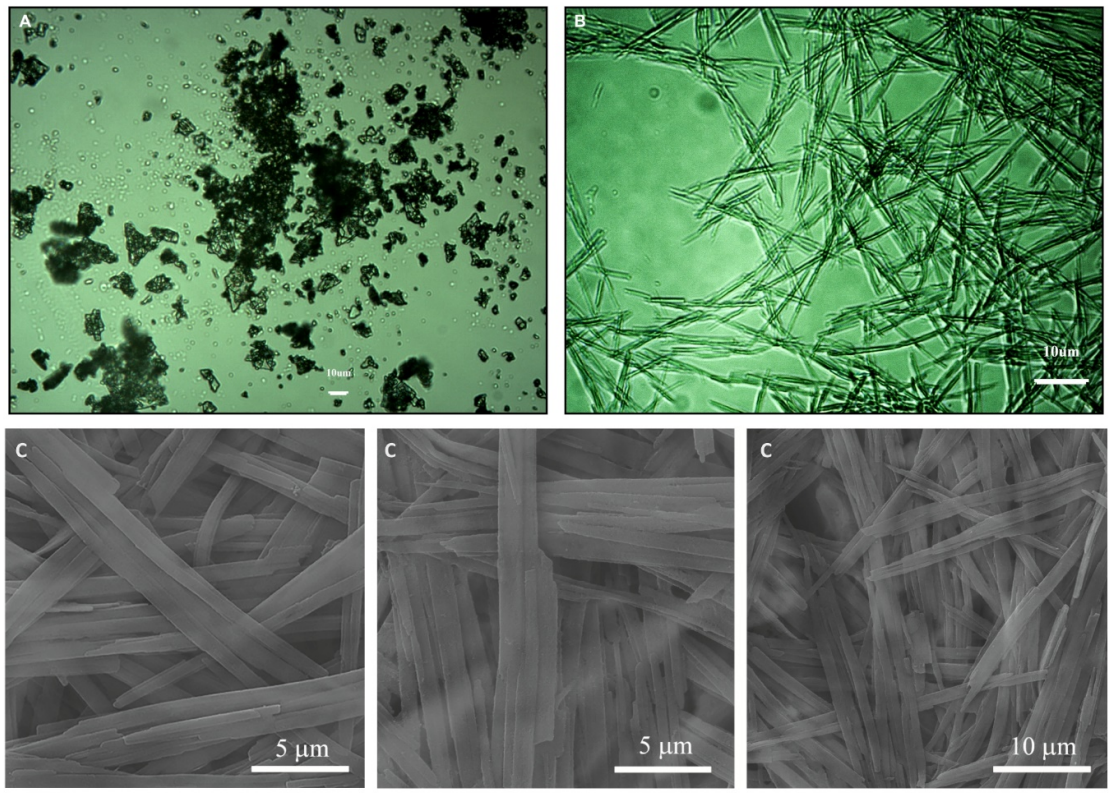

Figure 3. A-B) Representative light microscopy images of A) commercial resveratrol given here just for comparison purposes and B) of as-prepared nanobelt-like ResNPs obtained by solvent/non-solvent method (bar 10µm); C) Representative FESEM images of nanobelt-like ResNPs (bars 5 and 10µm)

Storage time did not affect the morphology of the particles in suspension, or powders. There was a macroscopically visible small intensity of precipitation in suspension following storage for more than 7 days, but it was easily dissolved by movement.

3.3. Artemia salina bioassay

The bioactivity of as-preparedResNPs was examined by *Artemia salina* bioassay. Survival of *Artemia* treated with 375 to 0.1 µg/ml of ResNPs suspension is shown in **Figure 4.** After 24hof treatment, only the highest concentrations of ResNPs suspension caused mortality of slightly over 20%, suggesting no toxicity prior to ingestion, and the absence of mechanical damage. At this point, all larvae have molted into the second larval phase. Survival after 48h was significantly lower for all concentrations above 10 µg/ml. This is consistent with the high sensitivity of the second larval phase of *Artemia*, when these organisms start filter feeding with particles from the environment, and is the most appropriate age for assays.[36] After 48h of treatment, LD_{50} was 31.89 µg/ml. It is considered that toxicity in *Artemia* expressed by LD_{50}<250 µg/mlindicates the presence of biological activity.[21] Furthermore, values of LD_{50}>20 µg/ml are considered safe for humans.[22] Toxicity of ResNPs on *Artemia salina* suggests considerable biological activity, while still in range of safe in terms of toxicity.

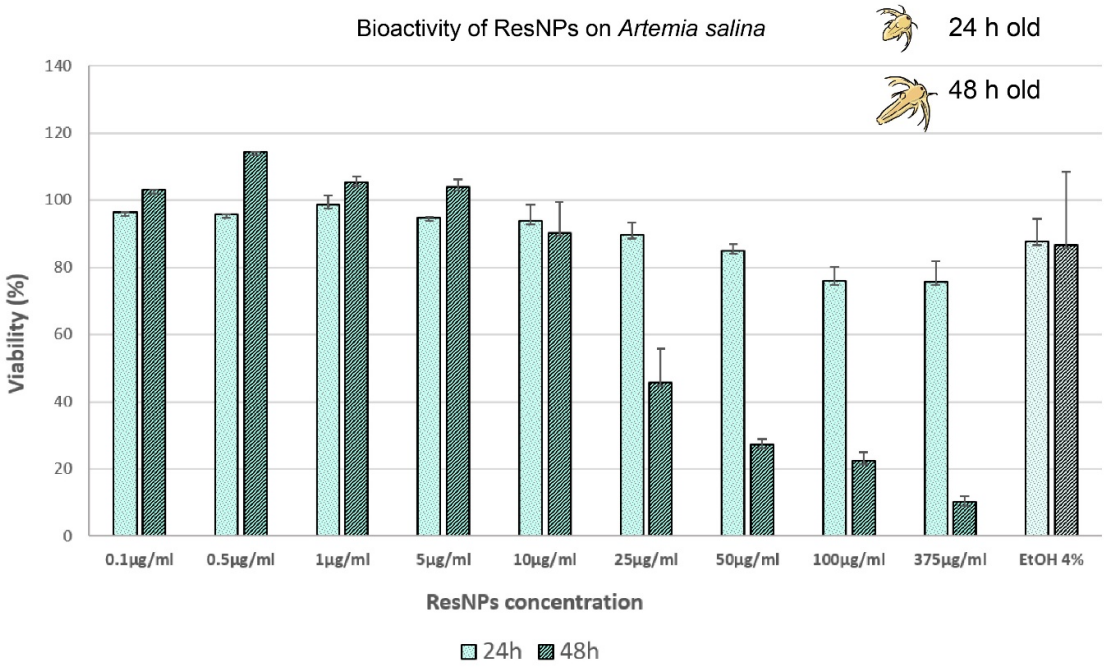

Figure 4. Bioactivity of ResNPs on *Artemia salina*

3.4. DPPH reductionassay

Resveratrol is known for its antioxidative activity, mainly based on the breakage of the OH bond.[37] Results of the DPPH assay confirming the antioxidative potential of ResNPs are presented in **Table 1**. Although both commercial resveratrol and ResNPs showed lower scavenging activity than vitamin C, the difference at higher concentrations was not pronounced. ResNPs possessed equivalent scavenging activity as commercial resveratrol when dissolved in methanol. In water, however, ResNPshad slightly better activity at 100 µg/ml and 1 µg/ml, but significantly higher activity was observed at aconcentration of 10 µg/ml.

Considering the results obtained from the physicochemical characterizations, the difference in the antioxidative activity can be attributed to the better solubility and dispersity of the resveratrol in the nanoform. At higher concentrations, the critical number of solvated resveratrol molecules was achieved in both samples, and the difference in the antioxidative activity diminished.

Incorporated antioxidants can reduce ROS around tissue scaffold, but fast diffusion of the antioxidative component from the scaffold is associated with negative effects on bone cells.[13] Good dispersity of ResNPs, rather than instantaneous complete dissolution, could be the basis for the achievement of local and sustained effect.

Table 1. ***DPPH scavenging activity (%)***

Mean ± S.E.

	1 mg/ml	100 μg/ml	10 μg/ml	1 μg/ml
Ascorbic acid (methanol)	**84.79** ± 1.18	**83.39** ± 2.66	**84.58** ± 1.56	**29.24** ± 9.25
ResNPs (methanol)	**80.74** ± 0.92	**80.12** ± 0,67	**61.67** ± 2,69	**14.08** ± 0.97
Res Commercial (methanol)	**81.26** ± 1.33	**79.76** ± 2.01	**54.08** ± 6.87	**9.69** ± 3.07
ResNPs (water)	/	**43.22** ± 2.32	**47.66** ± 1.96*	**23.58** ± 2.17
Res Commercial (water)	/	**38.79** ± 4.94	**34.43** ± 5.76*	**12.03** ± 13.02

* = Statisticalysignifficant difference between ResNPs and ResCommercial (*p* value <0.05)

3.5. Microdilution assay

Prescreening of the antibacterial properties of ResNPs was done by the microdilution assay and resazurin stain. These results are listed in **Table 2**. and they indicate notable antibacterial potential. Obtained results indicate that ResNPs inhibited bacterial growth at concentrations of 800 μg/ml in cases of *Staphylococcus aureus* and *Staphylococcus epidermidis*, both ATCC and clinical strains. These results are especially significant because these Gram-positive strains are considered to be the major causes of orthopedic infections.[28] In addition, MIC value was also 800 μg/ml in the case of aclinical isolate of *Pseudomonas aeruginosa*, which was not sensitive to commercial resveratrol. This difference can be related to thespecific physical form and mechanism of action of ResNPs particles, allowing astronger effect on this strain.However,ResNPsdid not significantly affect other tested bacteria at this concentration range. MBC of ResNPs for *Staphylococci* and clinical strain of *P. aeruginosa*was shown to be higher than MIC value.

Table 2. ***MIC and MBC values***

Bacterial strain	MIC values ResNPs	MIC values commercial resveratrol	MBC ResNPs	MBC commercial resveratrol	MIC streptomycin
Staphylococcus aureus ATCC 29213	800 µg/ml	800 µg/ml	>800 µg/ml	>800 µg/ml	3.125 µg/ml
Staphylococcus aureus clinical isolate	800 µg/ml	800 µg/ml	>800 µg/ml	>800 µg/ml	3.125 µg/ml
Staphylococcus epidermidis ATCC 12228	800 µg/ml	800 µg/ml	>800 µg/ml	>800 µg/ml	1.5 µg/ml
Staphylococcus epidermidis clinical isolate	800 µg/ml	800 µg/ml	>800 µg/ml	>800 µg/ml	1.5 µg/ml
Escherichia coli ATCC 35218	>800 µg/ml	>800 µg/ml	NA	NA	>100 µg/ml
Escherichia coli clinical isolate	>800 µg/ml	>800 µg/ml	NA	NA	>100 µg/ml
Pseudomonas aeruginosa ATCC 27853	>800 µg/ml	>800 µg/ml	NA	NA	100 µg/ml

Pseudomonas aeruginosa clinical isolate	800 µg/ml	>800 µg/ml	>800 µg/ml	NA	>100 µg/ml
Enterococcus faecalis ATCC 29212	>800 µg/ml	>800 µg/ml	NA	NA	25 µg/ml
Proteus mirabilis ATCC 29906	>800 µg/ml	>800 µg/ml	NA	NA	25 µg/ml

Values of a minimal inhibitory concentration of resveratrol on each of these bacteria vary in the literature. For example, resveratrol exhibited MIC of 100 µg/ml on S*taphylococcus aureus* ATCC 25923,[38] but more than 1000 µg/ml on the same strain.[39]*Staphylococcus epidermidis* ATCC 12228was not sensitive to resveratrol at 1000 µg/ml, in the work of Jung et al.,[39] but data about resveratrol effect on these bacteria is scarce. Our results support the factthat *Staphylococci* express sensitivity to resveratrol within a certain range. This is a promising finding in terms of the possible use of ResNPs in tissue scaffolds engineering, due to the burden of *Staphylococcus aureus* and *Staphylococcus epidermidis* implant infections.[27] There are also various results recorded previously for resveratrol regarding bacteria not sensitive to ResNPs in our study. Jung et al.[39]reported different sensitivity of *E. coli* strains ATCC 47004 and ATCC 25922, with MIC values of250 and 1000 µg/ml, respectively. *P. aeruginosa* ATCC 27853 strain and clinical isolate exhibited MIC values > 400µg/ml,[38] in previous literature. *Pseudomonas aeruginosa* PAO1 169 showed MIC values >1000 µg/ml.[39]*Enterococcus faecalis* ATCC 29212 was sensitive at 100 µg/ml,[38] but different MIC

values of resveratrol for *E. faecalis* are also mentioned.[18] *Proteus mirabilis* ATCC 7002 was not sensitive to resveratrol at 1000 μg/ml.[39] From our results and literature data, it could be concluded that resveratrol demonstrates an inhibitory effect on bacteria, but it is largely dependent on the bacterial strain and possibly experimental and other factors.[18] These observations also mean the possibility of improvement of effect by varying certain properties of pure resveratrol particles. Although the antimicrobial effect tested by exposure in liquid medium gave us preliminary information about this aspect of our material, in the context of tissue engineering and bioglass-coating materials, other antibacterial effects such as antibiofilm, coated surface effect, and others will be tested in our further research.

3.6 ResNPs coating of bioactive glass-based scaffold

The coating of bioglass scaffolds has proven as a promising strategy in the past, particularly when the goal is achieving enhanced biological properties. The number of materials aimed for this purpose is constantly growing but the issue that remains challenging is efficient coating without impairing the specific porous structure of the scaffolds. Here we have tested the potential application of ResNPs for the coating of bioactive glass-based scaffolds. Coated scaffolds were characterized by FTIR spectroscopy and optical microscopy to confirm the presence of resveratrol on the scaffold's surface and to investigate the possible interaction between them (**Figure 5**).

Based on the FTIR characterization, the bands characteristic for both materials are detected in the spectrum of the coated scaffold (**Figure5A**). Besides previously mentioned bands of ResNPs, these are the bands that originated from bioglass (Si-O-Si and Si-O bands at 1024, 926, and 480 cm^{-1} and bands at 560 and 600 cm^{-1} which correspond to P-O bending

vibrations of crystalline phosphates).[40] For better comparison, the spectra of the uncoated scaffold and ResNPs are given in the same graph. Significant shifting or changes in the appearance of peaks were not detected, indicating that ResNPs did not interact with the surface of scaffolds and presumably only physically attached to it. Thus, thechemical reactivity of resveratrol was preserved.

Scaffolds coated with ResNPs exhibited a change of color (macroscopic observation inserts in **Figure 5A** and microscopic **B and C**). Microscopic analysis (**Figure 5 B, B', C, and C'**) revealed that the coating was uniform, with layers of ResNPs forming over the struts of the scaffolds. In some rare cases, ResNPs formed membranes over the pores of the scaffold. It seems that rotation of the glass vessel prevented the gravity-driven separation of ResNPs on the bottom side of the scaffolds and contributed to a homogeneous distribution of the nanobelts on the surface of scaffolds struts. In addition, we are assuming that this distinct morphology and the size of ResNPspromotedeffective attachment on the struts, with a low probability of pore clogging.

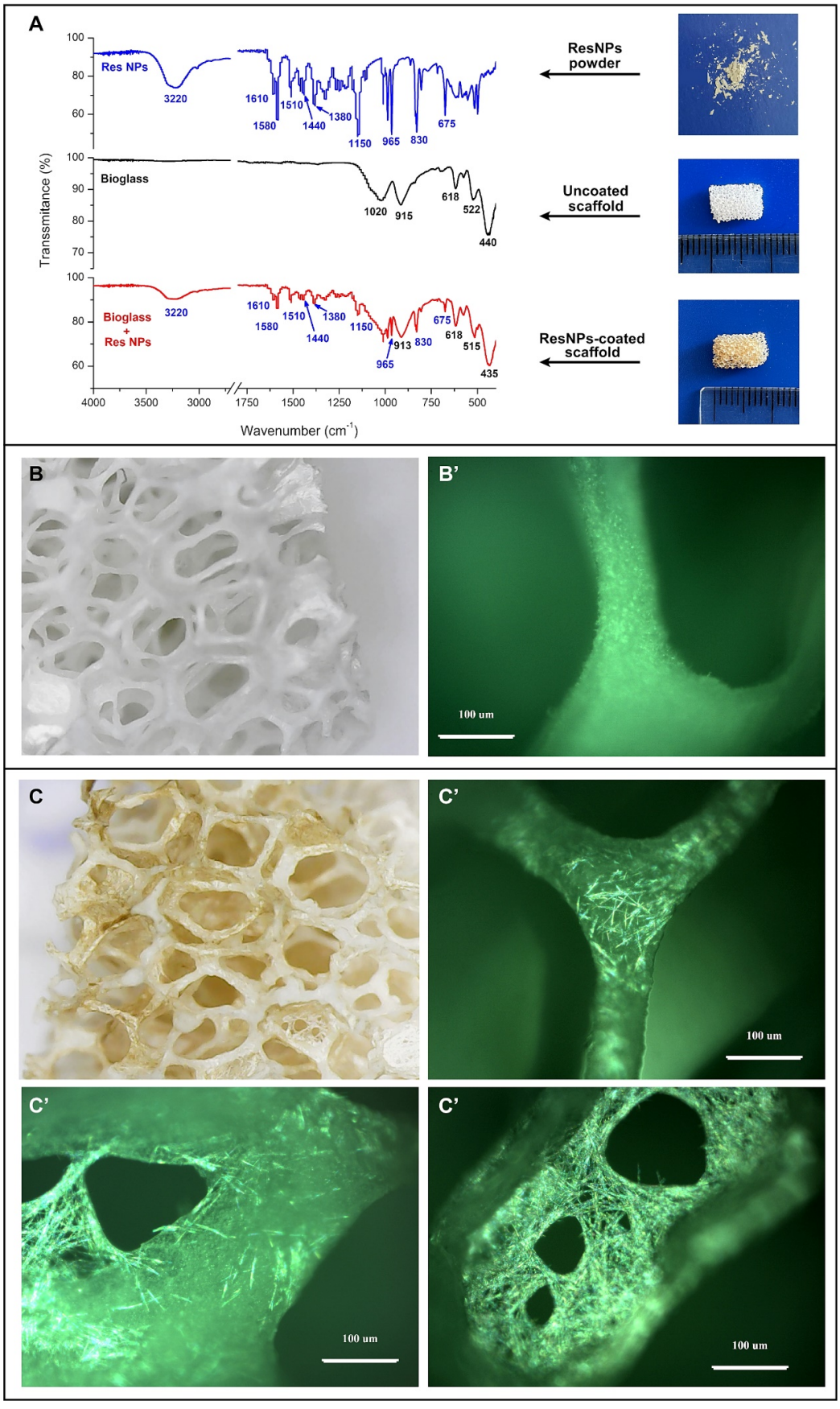
A
Res NPs
3220
1610
1580
1510
1440
1380
1150
965
830
675
Bioglass
1020
915
618
522
440
Bioglass
+
Res NPs
3220
1610
1580
1510
1440
1380
1150
965
913
830
675
618
515
435
Transmittance (%)
Wavenumber (cm-1)
ResNPs
powder
Uncoated
scaffold
ResNPs-coated
scaffold
B
B'
C
C'
C'
C'
100 um
100 um
100 um
100 um

Figure 5. FTIR spectra of ResNPs, coated and uncoated scaffold (A). Inserts in Fig. A represent macroscopic images of ResNPS powder, uncoated, and ResNPs coated scaffolds. Digital microscope observation of uncoated (B) and coated scaffold (C). Representative light microscopy images of uncoated (B') and coated scaffolds (C') (bars 100 μm).

4. Conclusions

In this research, we produced resveratrol nanobelt-like particles using the simple and green method of synthesis. SEM and optical microscopy revealed nanobelt-like morphology and uniformity of the particles. Particles were easily dispersed in water. UV-Vis was used to monitor ResNPs suspension, showing good stability. FTIR confirmed chemical composition and stability, and XRD showed structural characteristics. Nanobelt-like particles had high bioactivity, as suggested by *Artemia salina* assay, and effective antioxidative potential, even in water, asshown by DPPH assay. The antibacterialeffect was assessed on several species, revealing the inhibitory effect of ResNPs on *Staphylococcus aureus*, *Staphylococcus epidermidis,* and clinical isolate of *Pseudomonas aeruginosa*, although the concentration range used was not sufficient for significant inhibition of other tested pathogens. ResNPs have shown good potential for implementation in bioactive glass-based scaffold design. These results show a promising starting point for developing material based on resveratrol nanobelt-like particles with a combination of desirable properties in one device. Bioactive, antioxidative, antibacterial, stable, uniform nanobelt-like ResNPs will provide a strong foundation for the application of scaffolds in tissue engineering and better meet the needs in the healing process.

Conflict of Interest

The authors declare that the research was conducted in the absence of any commercial or financial relationships that could be construed as a potential conflict of interest.

Author Contributions

NT: Conceptualization, Data curation, Formal analysis, Investigation, Methodology, Writing – Original draft preparation. **TM:** Data curation, Formal analysis, Investigation, Methodology. **NF:** Methodology, Validation, Writing – Original draft preparation, Reviewing, and Editing. **DMĆ**: Methodology, Validation, Writing – Reviewing and Editing. **ARB:** Funding acquisition, Project administration, Resources, Writing –Reviewing and Editing **MMS:** Conceptualization, Investigation, Methodology, Funding acquisition, Project administration, Resources, Supervision, Writing – Original draft preparation, Reviewing and Editing.

Funding

Funds for the realization of this work were provided by the Ministry of Education, Science and Technological Development of the Republic of Serbia, Agreement on realization and financing of scientific research work of the Institute of Technical Sciences of SASA in 2022 (Record number: 451–03-68/2022–14/200175) and as a part of bilateral collaboration between the Republic of Serbia (MESTD) and Germany funded by the German Academic Exchange Service (DAAD). The work is also supported by MoESTD through Grant No: 451–03-68/2022–14/200178.

Acknowledgment

We thank Dr. LjiljanaVeselinović for the support in XRD measurements. We also thank Dr. Ina Gajic for providing bacteria from reference collection and clinical isolates for testing of antimicrobial activity.

Data Availability Statement

The datasets generated for this study are available upon request from corresponding authors.

References

1. Patel HM, Patel BB, Shah CN, et al. Nanosuspension technologies for delivery of poorly soluble drugs - A review. *Res J Pharm Technol* 2016; 9: 625–632.
2. Chung IM, Subramanian U, Thirupathi P, et al. Resveratrol nanoparticles: A promising therapeutic advancement over native resveratrol. *Processes* 2020; 8: 1–30.
3. Tian B, Liu J. Resveratrol: a review of plant sources, synthesis, stability, modification and food application. *J Sci Food Agric* 2020; 100: 1392–1404.
4. Zupančič Š, Lavrič Z, Kristl J. Stability and solubility of trans-resveratrol are strongly influenced by pH and temperature. *European Journal of Pharmaceutics and Biopharmaceutics* 2015; 93: 196–204.
5. Santos AC, Pereira I, Pereira-Silva M, et al. Nanotechnology-based formulations for resveratrol delivery: Effects on resveratrol in vivo bioavailability and bioactivity. *Colloids Surf B Biointerfaces* 2019; 180: 127–140.
6. Linh NTB, Lee BT. Electrospinning of polyvinyl alcohol/gelatin nanofiber composites and cross-linking for bone tissue engineering application. *J Biomater Appl* 2012; 27: 255–266.
7. Riccitiello F, De Luise A, Conte R, et al. Effect of resveratrol release kinetic from electrospun nanofibers on osteoblast and osteoclast differentiation. *EurPolym J* 2018; 99: 289–297.
8. Lin YC, Hu SCS, Huang PH, et al. Electrospun resveratrol-loaded polyvinylpyrrolidone/cyclodextrin nanofibers and their biomedical applications. *Pharmaceutics* 2020; 12: 1–16.

9. Zhang X, Han L, Sun Q, et al. Controlled release of resveratrol and xanthohumol via coaxial electrospinning fibers. *J Biomater Sci Polym Ed* 2020; 31: 456–471.

10. Ha ES, Park H, Lee SK, et al. Pure Trans-resveratrol nanoparticles prepared by a supercritical antisolvent process using alcohol and dichloromethane mixtures: Effect of particle size on dissolution and bioavailability in rats. *Antioxidants* 2020; 9: 1–16.

11. Jangid AK, Patel K, Jain P, et al. Carrier-free resveratrol nanoparticles: Formulation development, In-vitro anticancer activity, and oral bioavailability evaluation. *Mater Lett* 2021; 302: 130340.

12. Zhang X, Li Z, Yang P, et al. Polyphenol scaffolds in tissue engineering. *Mater Horiz* 2021; 8: 145–167.

13. Gao X, Xu Z, Liu G, et al. Polyphenols as a versatile component in tissue engineering. *Acta Biomater* 2021; 119: 57–74.

14. Valentino A, Di Cristo F, Bosetti M, et al. Bioactivity and delivery strategies of phytochemical compounds in bone tissue regeneration. *Applied Sciences (Switzerland)*; 11. Epub ahead of print 2021. DOI: 10.3390/app11115122.

15. Li J, Xin Z, Cai M. The role of resveratrol in bone marrow-derived mesenchymal stem cells from patients with osteoporosis. *J Cell Biochem* 2019; 120: 16634–16642.

16. Bo S, Gambino R, Ponzo V, et al. Effects of resveratrol on bone health in type 2 diabetic patients. A double-blind randomized-controlled trial. *Nutr Diabetes*; 8. Epub ahead of print 2018. DOI: 10.1038/s41387-018-0059-4.

17. Abedini E, Khodadadi E, Zeinalzadeh E, et al. A Comprehensive Study on the Antimicrobial Properties of Resveratrol as an Alternative Therapy. *Evidence-Based Complementary and Alternative Medicine* 2021; 2021: 1–15.

18. Vestergaard M, Ingmer H. Antibacterial and antifungal properties of resveratrol. *Int J Antimicrob Agents* 2019; 53: 716–723.

19. Liu F, Wei B, Xu X, et al. Nanocellulose-Reinforced Hydroxyapatite Nanobelt Membrane as a Stem Cell Multi-Lineage Differentiation Platform for Biomimetic Construction of Bioactive 3D Osteoid Tissue In Vitro. *Adv Healthc Mater* 2021; 10: 1–14.

20. Jin L, Guo X, Gao D, et al. NIR-responsive MXene nanobelts for wound healing. *NPG Asia Mater*; 13. Epub ahead of print 2021. DOI: 10.1038/s41427-021-00289-w.

21. Martins FJ, Senra M, Caneschi CA, et al. New group of azastilbene analogs of resveratrol: Synthesis, anticandidal activity and toxicity evaluation. *J King Saud Univ Sci* 2019; 31: 158–163.

22. Khaleel RI. Bio-toxicity study of some selected plant by Artemia salina (Leach) test. *Plant Arch* 2019; 19: 2847–2850.

23. Rajabi S, Ramazani A, Hamidi M, et al. Artemia salina as a model organism in toxicity assessment of nanoparticles. *DARU, Journal of Pharmaceutical Sciences* 2015; 23: 1–6.

24. Sorgeloos P, Remiche-Van Der Wielen C, Persoone G. The use of Artemia nauplii for toxicity tests-A critical analysis. *Ecotoxicol Environ Saf* 1978; 2: 249–255.

25. Finney DJ. Probit Analysis. *J Inst Actuar* 1952; 78: 388–390.

26. Moon J-K, Shibamoto T. Antioxidant assays for plant and food components. J Agric Food Chem. *Bioactive Food Proteins and Peptides: Applications in Human Health* 2009; 57: 1655–1666.

27. Oliveira WF, Silva PMS, Silva RCS, et al. Staphylococcus aureus and Staphylococcus epidermidis infections on implants. *Journal of Hospital Infection* 2018; 98: 111–117.

28. Stevanović M, Filipović N, Djurdjević J, et al. 45S5Bioglass®-based scaffolds coated with selenium nanoparticles or with poly(lactide-co-glycolide)/selenium particles: Processing, evaluation and antibacterial activity. *Colloids Surf B Biointerfaces* 2015; 132: 208–215.

29. Domokos R-A, Chiş V. Conformational Space and Electronic Absorption Properties of the Two Isomers of Resveratrol. *Studia Universitatis Babeș-BolyaiPhysica* 2017; 62: 43–61.

30. Allan KE, Lenehan CE, Ellis A V. UV light stability of α-cyclodextrin/resveratrol host-guest complexes and isomer stability at varying pH.*Aust J Chem* 2009; 62: 921–926.

31. Billes F, Mohammed-Ziegler I, Mikosch H, et al. Vibrational spectroscopy of resveratrol. *Spectrochim Acta A Mol BiomolSpectrosc* 2007; 68: 669–679.

32. Savic Gajic IM, Savic IM, Nikolic V, et al. The improvement of photostability and antioxidant activity of trans-resveratrol by cyclodextrins. *Advanced Technologies* 2017; 6: 18–25.

33. Chadha R, Dureja J, Karan M. Tempering trans-Resveratrol from the Molecule to Crystal Level: A Contemporary Approach toward Polymorphic Pursuits and Morphological Insights. *Cryst Growth Des* 2015; 16: 605–616.

34. Hilfiker R, von Raumer M (eds). *Polymorphism in the Pharmaceutical Industry: Solid Form and Drug Development*. : Weinheim, Germany, 2009.

35. Blagden N, de Matas M, Gavan PT, et al. Crystal engineering of active pharmaceutical ingredients to improve solubility and dissolution rates. *Adv Drug Deliv Rev* 2007; 59: 617–630.

36. Barahona M V., Sánchez-Fortún S. Comparative sensitivity of three age classes of Artemia salina larvae to several phenolic compounds. *Bull Environ ContamToxicol* 1996; 56: 271–278.

37. Phan Thi T, NinhThe S. Antioxidant of Trans -Resveratrol: A Comparison between OH and CH Groups Based on Thermodynamic Views. *J Chem*; 2020. Epub ahead of print 2020. DOI: 10.1155/2020/8869023.

38. Paulo L, Ferreira S, Gallardo E, et al. Antimicrobial activity and effects of resveratrol on human pathogenic bacteria. *World J MicrobiolBiotechnol* 2010; 26: 1533–1538.

39. Jung CM, Heinze TM, Schnackenberg LK, et al. Interaction of dietary resveratrol with animal-associated bacteria. *FEMS Microbiol Lett* 2009; 297: 266–273.

40. Boccaccini AR, Chen Q, Lefebvre L, et al. Sintering, crystallisation and biodegradation behaviour of Bioglass®-derived glass-ceramics. *Faraday Discuss* 2007; 136: 27–44.